Statistical, collective, and critical phenomena of classical one-dimensional disordered Wigner lattices

Shimul Akhanjee* and Joseph Rudnick†
Department of Physics, UCLA, Box 951547, Los Angeles, California 90095-1547, USA
(Received 25 April 2007; revised manuscript received 23 July 2007; published 26 October 2007)

We explore various properties of classical one-dimensional Wigner solids in the presence of weak disorder at $T=0$ in the context of a recently discovered Anderson transition of plasma modes in a random potential system. The extent to which the Wigner lattice is really a "crystal" rather than an amorphous solid is discussed for two types of disorder. The probability density of particle spacings is examined analytically within a weak disorder approximation and compared to numerical calculations for two different realizations of disorder. Regarding the plasma oscillations, the exact plasmon dispersion relations for the ordered Wigner crystal is derived analytically from the real space equations of motion. The methods introduced for performing the necessary lattice sums can be extended to tight-binding models of noninteracting electrons with power law hopping. We also discuss other quantities that follow from plasma oscillations such as the multifractal eigenfunctions, the compressibility of the electrons, and the ac conductivity.

DOI: 10.1103/PhysRevB.76.165129 PACS number(s): 71.23.−k, 63.22.+m, 63.50.+x, 72.15.Rn

I. INTRODUCTION

In 1934, Wigner predicted that an electron gas in a positive jellium background would, at low density, solidify into an ordered lattice.[1] Moreover, in classical systems that have been studied in certain soft condensed matter models, the strong Coulomb repulsion is sufficient to cause a system of particles to crystallize.[2] It is important to emphasize that the inclusion of strong disorder either chemically or, in the case of a low-dimensional system, via a rough external substrate will result in the destruction of a well-defined base lattice. That is, the term "Wigner crystal" is no longer entirely descriptive in the presence of sufficiently strong disorder. Rather, that system is closer to a "glass" than a crystalline solid.

Formally, the existence of Bragg peaks indicates that the system is a crystal. However, others have discussed the possibility that the system retains quasi-long-range order as a consequence of disorder.[3] Subtle implications are entailed by the term "glass" in describing a system in terms of its magnetic and topological properties. Here, we restrict our definition of "glasslike" to a system with a random positional configuration at zero magnetic field, even though a 1D system cannot truly be topologically disordered as in higher-dimensional systems.[4]

In any version of the Wigner crystal—or alternatively the "Wigner glass"—the most natural dynamical quantities to consider are the elementary excitations. The charged collective modes or plasmons at $T=0$ are entities of this sort, the essential features of which are captured by a classical description.[5] These quantities play an important role in the low-temperature thermodynamics and in the dynamical response of the system.

In this article we focus on two aspects of one-dimensional disordered Wigner crystal (1DWC) systems: in particular the plasma oscillations and the statistical behavior of the equilibrium electron locations. The effects of long-range interactions are often neglected in many discussions of Wigner crystals even though one would expect in real physical systems a complete breakdown of screening. So far, the complete plasmon dispersion and more importantly, its precise long wavelength behavior has not been deduced analytically. We present a simple derivation of the plasmon dispersion relation in a 1D Wigner crystal phase that exploits the summability properties of power law interactions that are unique to 1D systems. Moreover, the correct behavior of the two-dimensional (2D) longitudinal eigenmode is also calculated exactly by performing the most dominant single summation contribution, of which produces excellent agreement with known numerical results. Additionally, as an example of the utility of this form of analysis and owing to a similar mathematical structure we also apply these methods to calculate the band structure of an electronic tight-binding model with power law interactions, which is presented in an appendix. Furthermore, we numerically study the plasma modes of the disordered system and calculate the compressibility and the ac conductivity. Regarding the structural properties, we consider whether the distribution of the spacings between adjacent electrons can be analytically understood in terms of the randomness in other parameters in the Hamiltonian. A mathematical formalism is developed that provides some insight into the connection between the power spectrum of the randomness and the positional statistics. We also attempt to address the long-standing issue of whether a classical Wigner crystal in the presence of either random field or random charge disorder preserves some degree of crystalline integrity.

The organization of the rest of the paper is as follows. In Sec. II we discuss important aspects of the influence of disorder on the spacings between charged particles in a one-dimensional system. Two types of disorder are considered: one in which the randomness resides in the charges and the other in which it is the result of an external potential. Details of one approximate approach to this problem are contained in Appendix A. In Sec. III we report on the results of the numerical relaxation of the charges to their positions of mechanical equilibrium. Section IV contains a discussion of the extent to which disorder is destructive to crystalline order as measured by the amplitude of Bragg peaks. In Sec. V we discuss the dispersion relations and localization properties of

 ©2007 The American Physical Society

the plasma modes in both the ordered and the disordered systems. Finally, in Sec. VI we review the results reported and speculate on the experimental consequences of the effects considered in this article. Appendix B details Ewald summations utilized in our calculations and Appendix C contains results for the band structure of an electron system with power-law hopping, a by-product of our investigation of the dispersion relations for ordered systems with power-law interactions.

II. THE STATISTICAL CONFIGURATION OF THE PARTICLES UNDER THE INFLUENCE OF WEAK DISORDER

Let us now consider how disorder can affect the positional ordering of the particles in the 1DWC system. Evidently, the nature of disorder in such a system is not unique. It can exist in the spacings between the particle sites, the masses, the effective interaction between particles, or one can have a set of charges pinned by a random potential. It is also the case that the introduction of randomness in one parameter can induce randomness in another. For example, randomness in particle-particle interactions or an external field may well result in the destruction of a periodic base lattice at mechanical equilibrium.

The ordered system of size L is defined by the Hamiltonian

$$H = \sum_{i=1}^{L} \frac{p_i^2}{2m_e^*} + \frac{1}{2}\sum_{i\neq j} \frac{e_0^2}{|x_i - x_j|}, \tag{2.1}$$

where the quantities p_i and m_e^* refer to the momentum and effective mass of the ith particle, respectively. Our system lives in the low density regime in which the Coulomb interactions are much more influential than the kinetic energy, resulting in the crystalline ordering of the particles with the spatial coordinates $\{x_i\}$ separated with lattice constant a. Moreover, the system is stabilized by a positive Jellium neutralizing background. We wish to examine the vibrational modes of the system taking into account the full electrostatic force acting on each charge.

One can add to this Hamiltonian a term representing the interaction of the charges with a random electrostatic potential $V(x)$, defined as

$$V(x) = J\sum_{n}^{N} a_n \cos(2\pi n x) + b_n \sin(2\pi n x), \tag{2.2}$$

where the parameter J is a dimensionless coupling constant. The random variables a_n and b_n have a mean equal to zero. Moreover, their distributions are controlled by independent Gaussian distributions, the widths of which are independent of n, yielding a "white noise" power spectrum. We will call this system model A.

Additionally, we can explicitly inject randomness into the single charge values Q_i. We term this random charge system model B, where the Hamiltonian is obtained from Eq. (2.1) by replacing the e_0^2 with $Q_i \times Q_j$. Some possible realizations of this model may be found in soft condensed matter systems such as in biopolymer arrays that have contain randomly assigned chemical constituents and unscreened Coulomb interactions.[2]

In both models A and B, the charges in our lattice will relax to mechanical equilibrium, at locations that differ from the evenly spaced positions they occupy in the ordered case. Here, we characterize key properties of the equilibrium configuration, focusing on the statistical characteristics of the spacings between neighboring points. Finally, we discuss the extent to which the resulting lattice exhibits crystalline order.

As a first step in answering these questions for model B, we examine the product density functions for different distributions of charges, for three different realizations of the model: first when the individual charges are evenly distributed over a finite interval, second in which the charges randomly take on one of two discrete values and third, a random charge model in which the distribution of possible charges is Gaussian. This is done in Appendix A. There is a direct relationship between this distribution and the distribution of forces in the case of strongly screened interactions. The general distribution of the forces on a particular charge when interactions are unscreened requires a more involved analysis. Given this probability distribution, we turn to the distribution function of the spacings between the charges at equilibrium. It turns out that an analytical result that is valid in the weak disorder regime—based on the assumption that the width of the single charge distributions is very small—agrees remarkably well with the results of numerical calculations. We will call this result the "viscosity approximation" in that it is based on the notion that the charges will deviate from the ordered lattice by distances that are proportional to the total force acting on each charge $F_i^{\text{tot}} \propto \Delta x_i$ when they are equally spaced. That is, $P(F_i^{\text{tot}}) \propto P(\Delta x_i)$, as if the system were placed in a highly viscous medium and initial displacements of the charges from their initial positions were predictive of their eventual positions. Given this assumption, one can work out the solution to model B for all three of the distributions noted above starting with the Gaussian system.

The distribution of forces on the ith charge is given by the convolution

$$P_F(F_i) = \int_{-\infty}^{\infty} P_E(E_i) P_q(q_i)\, \delta(Eq - F_i) dE_i dq_i$$

$$= \int_{-\infty}^{\infty} P_E(F_i q_i) P_q(q_i) \frac{dq_i}{|q_i|}. \tag{2.3}$$

We must first determine $P_E(E_i)$, which describes the likelihood that a given charge will have an electric field acting on it. The total electric field acting on the ith charge is $E_{\text{total}}^i = \sum_{i\neq j} q_j \xi_{i,j}$, where $\xi_{ij} \approx \frac{1}{(x_i - x_j)^2}$. Subsequently, if we examine the first charge in the array, the distribution of electric fields acting on it is a distribution governed by the convolution

$$P_E(E_1) = \int_{-\infty}^{\infty} dq_2 \int_{-\infty}^{\infty} dq_3 \cdots \int_{-\infty}^{\infty} dq_N P_q(q_2) P_q(q_3) \cdots P_q(q_N)$$

$$\times\, \delta(q_2\xi_{2,1} + q_3\xi_{3,1} + \cdots + q_N\xi_{N,1} - E_1). \tag{2.4}$$

This convolution can be simplified by making use of the Fourier representation of the Dirac delta function

$$\delta(q_2\xi_{2,1}+q_3\xi_{3,1}+\cdots+q_N\xi_{N,1}-E_1)$$
$$=\frac{1}{2\pi}\int_{-\infty}^{\infty}\exp[i\Omega(q_2\xi_{2,1}+q_3\xi_{3,1}+\cdots+q_N\xi_{N,1}-E_1)]d\Omega. \tag{2.5}$$

More generally, for any given charge, the distribution of the electric fields $P_E(E_i)$ is transformed into the following single integration:

$$P_E(E_i)=\frac{1}{2\pi}\int_{-\infty}^{\infty}e^{-i\Omega E_i}\left(\prod_{k\neq i}^{N}g_k(\Omega)\right)d\Omega, \tag{2.6}$$

where we have integrated out the charges by performing an integral that defines $g(k)$

$$g_k(\Omega)=\int_{-\infty}^{\infty}P_q(q_k)\exp[i\Omega q_k\xi_{k,i}]dq_k$$
$$=\exp[i\Omega\xi_{k,i}q_0-\xi_{k,i}^2\Omega^2\sigma/2]. \tag{2.7}$$

The resulting distribution of electric fields is in closed form

$$P_E(E_i)=\frac{1}{2\pi}\int_{-\infty}^{\infty}\exp\left[i\Omega\left(\sum_{k=1}^{N}\xi_{k,i}q_0-E_i\right)-\frac{\Omega^2\sigma}{2}\sum_{k\neq i}^{N}\xi_{k,i}^2\right]d\Omega$$
$$=\frac{\exp\left[-\left(\sum_{k=1}^{N}\xi_{k,i}q_0-E_i\right)^2\Big/\left(2\sigma\sum_{k\neq i}^{N}\xi_{k,i}^2\right)\right]}{\left(2\pi\sigma\sum_{k\neq i}^{N}\xi_{k,i}^2\right)^{1/2}}. \tag{2.8}$$

The distribution of the force can now be determined by using Eq. (2.3). As a consequence of the periodic boundary conditions we can take $\Sigma_{k\neq i}^{N}\xi_{k,i}=0$. Moreover, we can apply the exact sum $\Sigma_{r=1}^{\infty}1/r^2=\pi^2/6$ in the limit of a large system size to the $\xi_{k,i}^2$ summation, reducing Eq. (2.8) to a Gaussian distribution centered at zero:

$$P_E(E_i)=\frac{\exp[-3(E_i)^2/(\pi^2\sigma)]}{(\pi^3\sigma/3)^{1/2}}. \tag{2.9}$$

The resulting force distribution is simply a convolution of two Gaussian distributions

$$P_F(F_i)=\int_{-\infty}^{\infty}\frac{\exp[-3(F_i/q_i)^2/(\pi\sigma)-(q_i-q_0)^2/2\sigma]}{(\pi^2\sigma/3)^{1/2}|q_i|}dq_i. \tag{2.10}$$

We now turn to the other distribution functions. The system with uniform random charges, defined by the density function (A3) can also be evaluated. We can apply convolution of Eq. (2.3). Similar steps lead to the analysis of Eq. (2.7),

$$g_k(\Omega)=\int_{W_1}^{W_2}\frac{\exp[i\Omega q_k\xi_{k,i}]}{W_2-W_1}dq_k$$
$$=\frac{2\exp[i\Omega\xi_{k,i}(W_2+W_1)/2]\times\sin[\Omega\xi_{k,i}(W_2-W_1)/2]}{(W_2-W_1)\Omega\xi_{k,i}}. \tag{2.11}$$

After applying Eq. (2.4) we have

$$P_E(E_i)=\frac{1}{2\pi}\int_{-\infty}^{\infty}e^{-i\Omega E_i}\times\left(\prod_{k\neq i}^{N}\frac{e^{i\Omega\xi_{k,i}(W_1+W_2)/2}\sin[\Omega\xi_{k,i}(W_2-W_1)/2]}{\Omega\xi_{k,i}(W_2-W_1)/2}\right)d\Omega. \tag{2.12}$$

Similarly, for binary disorder we have

$$P_E(E_i)=\frac{1}{2\pi}\int_{-\infty}^{\infty}e^{-i\Omega E_i}\times\left(\prod_{k\neq i}^{N}e^{i\Omega\xi_{k,i}(Q_1+Q_2)/2}\cos[\Omega\xi_{k,i}(Q_2-Q_1)/2]\right)d\Omega. \tag{2.13}$$

This leads to the final force distributions for the uniform and the binary systems, respectively, as

$$P_F^{\mathrm{uni}}(F_i)=\int_{-\infty}^{\infty}\frac{Ei(-i\Omega F_i/W_1)-Ei(-i\Omega F_i/W_2)}{2\pi(W_2-W_1)}\times\left(\prod_{k\neq i}^{N}\frac{e^{i\Omega\xi_{k,i}(W_1+W_2)/2}\sin[\Omega\xi_{k,i}(W_2-W_1)/2]}{\Omega\xi_{k,i}(W_2-W_1)/2}\right)d\Omega \tag{2.14}$$

and

$$P_F^{\mathrm{bin}}(F_i)=\int_{-\infty}^{\infty}\left(\frac{\exp(-i\Omega F_i/Q_1)}{4\pi Q_1}+\frac{\exp(-i\Omega F_i/Q_2)}{4\pi Q_2}\right)\times\left(\prod_{k\neq i}^{N}e^{i\Omega\xi_{k,i}(Q_1+Q_2)/2}\cos[\Omega\xi_{k,i}(Q_2-Q_1)/2]\right)d\Omega, \tag{2.15}$$

where $Ei(x)$ is the exponential integral defined as

$$Ei(x)=-\int_{-x}^{\infty}\frac{e^{-t}dt}{t}. \tag{2.16}$$

The density of particle spacings is simply proportional to these force distributions.

This derivation in terms of probability convolutions can similarly be extended to the random potential system of model A. We previously defined the random potential in Eq. (2.2). To simplify the analysis we will only consider the cosine contributions and will perform the analysis for a Gaussian distribution of the random amplitudes. The resulting Fourier decomposition yields the expression

$$V(x)=\frac{1}{\sqrt{L}}\sum_{n=1}^{L}a_n\cos(n\pi x/L). \tag{2.17}$$

The force on the ith charge is then given by

$$F(x_i) = -e_0 V'(x)|_{x_i} = \frac{e_0}{L^{3/2}} \sum_{n=1}^{L} a_n (n\pi) \sin(n\pi x_i/L). \tag{2.18}$$

It is evident that the source of the randomness is not a coupling constant between particles as was the case in model B. Rather, we relate probability density of random Fourier amplitudes a_n ("white noise") to the particle probability density of successive spacings. The probability convolution for the force is given as

$$P(F_i) = e_0 \int_{-\infty}^{\infty} da_1 \int_{-\infty}^{\infty} da_2 \cdots \int_{-\infty}^{\infty} da_L P_a(a_1) P_a(a_2) \cdots P_a(a_L) \delta\left\{ \frac{\pi}{L^{3/2}} \left[a_1 \sin\left(\frac{\pi x_i}{L}\right) + 2a_2 \sin\left(\frac{2\pi x_i}{L}\right) \cdots L a_L \sin(\pi x_i) - F_i \right] \right\}. \tag{2.19}$$

As a consequence of Eq. (2.19) having the same mathematical structure as (2.4), one can carry out the same steps that lead to Eq. (2.8), yielding the expression

$$P(F_i) = \frac{e_0 \exp\left(-F_i^2 \Big/ \left\{ 2\sigma \sum_{n=1}^{L} \left[\frac{(n\pi)}{L^{3/2}} \sin\left(\frac{n\pi x_i}{L} \right) \right]^2 \right\} \right)}{\sqrt{\left\{ 2\sigma \sum_{n=1}^{L} \left[\frac{(n\pi)}{L^{3/2}} \sin(n\pi x_i/L) \right]^2 \right\}}}. \tag{2.20}$$

Our final result for the distribution of nearest neighbor spacings of model A is simply a Gaussian distribution with a width that depends on the relative spatial location x_i of any given particle. This corresponds to the same Gaussian distribution type as the random amplitudes a_n used to construct the random potential. However, the width differs, as the spacings distribution contains a width that is a function of the precise characteristics of the random potential.

In model B, one can naively compare all of the derived probability densities of nearest-neighbor spacings to the probability densities of force couplings given earlier by Eqs. (2.10), (2.14), and (2.15). The binary system contains three characteristic peaks in both determined density functions, showing similar qualitative behavior. Furthermore, in the Gaussian case both the force couplings and the nearest-neighbor spacings follow a convolution of two Gaussian distributions. On the other hand, for the uniform distribution the probability density of nearest-neighbor spacings does not follow the logarithmic behavior of the force couplings. Ultimately, this indicates the importance of the distribution type in detailing the equilibrium structural properties of 1DWC systems.

As remarked earlier, the viscosity approximation assumes that the particles will deviate from the ordered lattice by a displacement that is proportional to the total force on each particle when the particles are equally spaced. Although we cannot at the moment rigorously justify this assumption, nor can we can we formulate precise criteria for its validity, this approximation seems reasonable when the disorder is relatively weak compared to the interaction strength of the Coulomb force. However, it is necessary test this hypothesis by performing a numerical relaxation of the particles for both models A and B in finite sized systems. We detail the procedure and compare the numerical results to our previously derived expressions in the next section.

III. THE NUMERICAL RELAXATION OF THE PARTICLES TO EQUILIBRIUM

The numerical relaxation of a disordered 1DWC to its minimum energy configuration requires the development of two major components. First one must address the complications that arise from performing computations on finite size systems with long ranged interactions. Evidently, the surface effects, as a result of long range interactions in finite sized systems are not negligible. One possible route to dealing with this complication is to enforce periodic boundary conditions. The standard approach involves the Ewald summation technique.[6] We have derived our version of the Ewald potential displayed as Eq. (B2) in Appendix B, that represents the interaction energy between charges on a periodic image, of which is infinitely repeated to assert the periodic boundary conditions. However, the resulting rapidly converging sums still demand computationally intensive efforts. We have discovered that the summation can be substantially reproduced in closed form in terms of a simple function that exhibits the proper short distance behavior and also embodies the correct periodicity. Consider the lattice summation of the $1/R$ Coulomb potential representing the infinite sum of n images of length d. The interaction potential between two particles separated by a distance x within a image is given by the expression

$$\phi(x) = \left| \sum_{n=-\infty}^{\infty} \frac{(-1)^n}{(n + x/d)} \right| = \pi |\csc(\pi x/d)|. \tag{3.1}$$

The result is a simple trigonometric function, of which is easy to implement numerically. Figure 1 shows a graphical

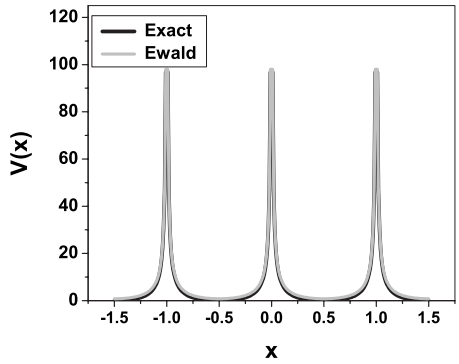

FIG. 1. A comparison of the exact and Ewald representations of the Coulomb interaction energy.

comparison of the expressions (B2) and (3.1).

Next we consider the other required numerical tool. An energy minimization algorithm is necessary to find the spatial coordinates at which the particles arrange themselves given a particular realization of disorder in the Hamiltonian. These coordinates satisfy a system of linear equations, namely the simultaneous zeros of the total force on each charge. A very powerful technique is the Newton-Raphson (NR) method.[7] In the NR method one recursively computes the Hessian or second derivative matrix and multiplies its inverse by the initial positions. The resulting product is used to increment the coordinates towards the equilibrium configuration. One interesting property of the Hessian matrix is that it is precisely the dynamical matrix one uses to compute the phonon spectrum of a vibrating lattice. In our 1DWC system, we can examine the plasma oscillations by simply diagonalizing the Hessian of a relaxed array of particles. Using the interaction potential of Eq. (3.1), the Hessian of a finite size lattice has the form[8]

$$\mathbf{D}(\mathbf{R}-\mathbf{R}') = \delta_{\mathbf{R},\mathbf{R}'} \sum_{\mathbf{R}''} \left. \frac{\partial^2 \phi(x)}{\partial x^2} \right|_{x=\mathbf{R}-\mathbf{R}''} - \left. \frac{\partial^2 \phi(x)}{\partial x^2} \right|_{x=\mathbf{R}-\mathbf{R}'}. \tag{3.2}$$

This yields an $N \times N$ matrix that can one use to carry out the standard phonon analysis. We have implemented numerical relaxations on chains of length $N=1024$, for each of the random charge and random field distributions discussed in the previous section. Numerical uncertainty exists in the amount of residual total force acting on a particular charge. Therefore, the charges were relaxed so that the residual forces were only about $\approx 10^{-6}$ in relative magnitude (scaled to unity), at which point our system is quite close to equilibrium. We have compared the theoretical predictions of the viscosity approximation given by Eqs. (2.14), (2.15), (2.10), and (2.20) to the numerical data in Figs. 2 and 3. We find excellent agreement between the viscosity approximation and numerical calculations in terms in the general behavior of all of the resulting distributions, with the exception of the binary case where the agreement is more at a qualitative level. Furthermore, it is clear that the statistical arrangement of the disorder has an explicit dependence on the distribution type and width. The qualitative correlation is quite striking in

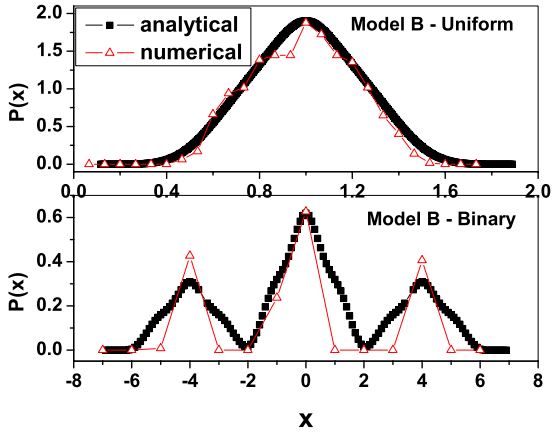

FIG. 2. (Color online) A comparison of the analytical and numerical distribution of nearest neighbor spacings in the case of Model B, in which the disorder is in the magnitude of the charges. The analysis is based on the viscosity approximation.

the case of the binary random charge system, where the three characteristic peaks are mirrored in both the numerical and analytical plots. Figure 2 should be taken as an illustration of the qualitative utility of the viscosity approximation and as an indication of the limits on the quantitative accuracy of that approach. In any case, our investigations suggest that an experimental probe of the structural arrangement of disordered systems with long-ranged interactions would reveal a pronounced difference between the chemically disordered binary system and the random potential system, of which represents a form of substrate disorder. It is also worth noting that the effect could also exist in several soft condensed matter models in which Wigner crystal ordering has been discussed in the context of biological systems.[2]

IV. CRYSTALLINE ORDER

It is well known that there is a strict absence of long range crystalline order for systems with short-ranged interactions

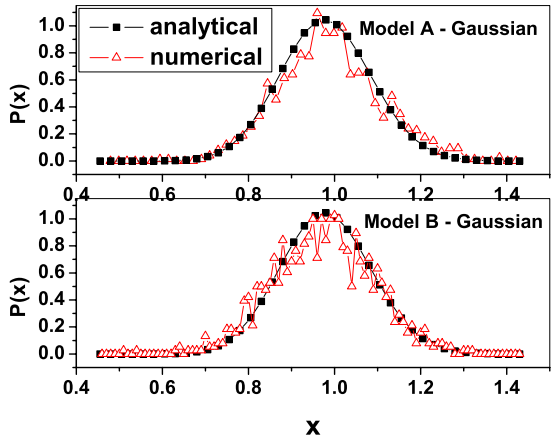

FIG. 3. (Color online) A comparison of the analytical and numerical distribution of nearest neighbor spacings in model A, in which the randomness derives from the external potential. The analysis is based on the viscosity approximation.

that exist in dimensions $d \leqslant 2$, resulting from the prevailing influence of thermal and quantum fluctuations. This notion has been explored by various authors.[9] For Wigner crystals in particular, the unscreened Coulomb interactions factor into these melting criteria through the precise wave vector dependence of the longitudinal and transverse vibrational modes that lead to diverging values of the Lindemann parameter $\langle u^2 \rangle$ in a low enough dimensionality.

As we have demonstrated in the preceding section, the inclusion of quenched disorder induces randomness in particle spacings. Furthermore, another main consequence of the disorder is that eigenmodes are not plane waves. However, as we will show in our investigation of the Bragg peaks, the Fourier space is not necessarily destroyed.

In our 1DWC system, let us isolate the role of quenched disorder in making the particle array more amorphous while neglecting the known effects of stochastic zero point disturbances studied by other authors.[10] Again, this is valid in systems in which Wigner-like ordering is present but those entropic contributions are suppressed. A more useful route to the exploration of the possibility of long range order involves the structure factor S_k, which can be defined in terms of the equilibrium positions of the ith particle x_i^{equ}:

$$S_k = \frac{1}{L}\left\langle \sum_{i=1}^{L} e^{ikx_i^{\mathrm{equ}}} \right\rangle, \quad k = \frac{2\pi n}{L}, \quad n = 1,2,3,\ldots . \tag{4.1}$$

The crystalline character of the system will manifest itself through the existence of at least one delta function, or Bragg peak, in the spectrum of S_k within some particular scale in Fourier space.

From the exact dispersion relation[11] of the clean 1D Wigner crystal $\omega(k) \sim |k| \ln^{1/2}(1/k)$, it has been shown that the correlation functions decay much slower than any power law $\langle [u(x)-u(0)]^2 \rangle \propto \sqrt{\ln(x)}$. The resulting prediction of strong Break peaks in a scattering experiment follows from the scattering intensity tending as $I(x) \propto \exp\{-A\langle [u(x)-u(0)]^2 \rangle\}$, of which is relatively slow compared to the typical, strong exponential decay observed in systems with short-ranged interactions. According to the literature, systems possessing this sort of decay are usually labeled as having "quasi-long-range order."[3]

The quantity S_k is calculated for numerically relaxed ensembles in both models A and B at different relative disorder strengths. In the case of model A, the disorder strength is the dimensionless combination $\kappa \equiv Q^2/J$ for values of J defined in Eq. (2.2), while for model B, it is simply the single charge distribution width $W = 1 + W_0(W_2 - W_1)$, where $W_0 = 0$ is the ordered case.

The S_k data is shown in Figs. 4 and 5. The plots suggest a difference between both models in terms of their structural properties. It appears that both models retain their crystalline composition for a regime of disorder strengths. Moreover, in the high disorder regime, the Bragg peaks are lost. The details of the transition will be examined more carefully in a future work. A notable difference between the systems is that in model A the Bragg peaks strongly resemble delta functions while in model B, the scattering intensity contains an exponentially broadened shoulder tending on both sides of the peak at higher disorder strengths, although the presence of peak shoulders in model B is not evident at low disorder. Hence for weak disorder both models are crystals based on the strictest definition requiring the existence of just one Bragg peak.

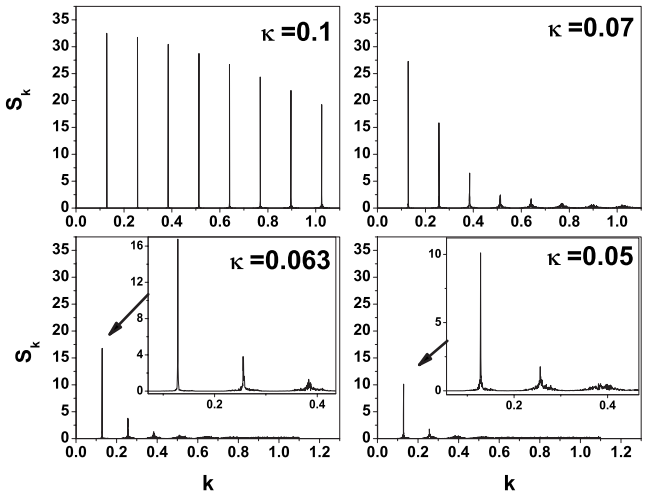

FIG. 4. S_k for different relative interaction strengths, model A, $L=256$. At high κ, or low disorder strength, in the delocalization critical regime, the system maintains the composition of the first Bragg peak, indicating the preservation of some sort of crystalline aspect to the system.

In order to appropriately make sense of Figs. 4 and 5 one should focus on the first Bragg peak and how it behaves as the disorder strength is increased. Evidently, the peak height decreases for both models as function of disorder strength. It is also worth noting that the peaks decrease across Fourier space according to a Debye-Waller damping envelope, tending as $I_{\mathrm{DW}} \sim \exp\{-\langle [qu(0)]^2 \rangle\}$. The precise reduction of the first Bragg peak height g was studied for both models and we determined a power law behavior of the peak height in terms of the disorder strength. We performed a linear fit shown in

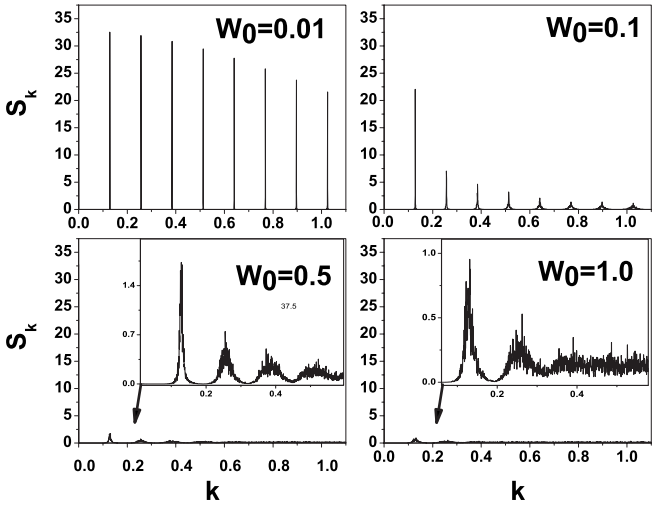

FIG. 5. S_k for different disorder strengths, model B, $L=256$.

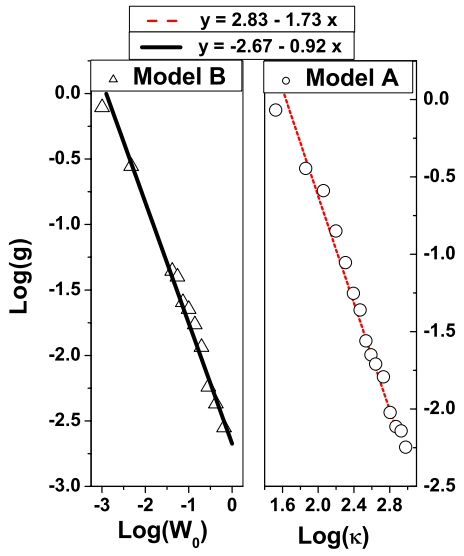

FIG. 6. (Color online) The behavior of the height of the first Bragg peak g for different disorder strengths.

Fig. 6 on a logarithmic scale yielding $g_A(\kappa) \sim \kappa^{-\alpha}$ and $g_B(W_0) \sim W_0^{-\beta}$, for values of $\alpha \approx -1.7272 \pm 0.0696$ and $\beta \approx -0.9217 \pm 0.0324$. Apparently, this power law behavior breaks down at higher disorder strengths, as the system becomes more amorphous.

V. THE PLASMA OSCILLATIONS

A. The ordered system

We first discuss the ordered system with a Hamiltonian described by Eq. (2.1). Others have investigated the normal modes of a similar system with screened (Yukawa) interactions between the charges with driving and dissipative terms.[12] However, we shall focus on the normal modes that follow from unscreened Coulomb interactions. The eigenvalue equation of interest follows directly from the classical equations of motion for the total force acting on each particle. This is given by the following expression:

$$-m_e\omega^2 u(x) + \sum_{x' \neq x} \phi_{x,x'} u(x') = 0, \tag{5.1}$$

where $u(x)$ is the displacement of a lattice site from equilibrium and

$$\phi_{x,x'} = 1/(x - x')^3 \tag{5.2}$$

is the electrostatic force constant between two particles in the array, of which is the second derivative of the interaction potential in the harmonic approximation. As a consequence of the periodic ordering and translational symmetry present in the system we can assume the eigenfunctions have the form

$$u(na) \propto \exp[i(kna - \omega t)] \tag{5.3}$$

of which k is the Fourier component and $n=1,2,3,\ldots$. We substitute Eqs. (5.2) and (5.3) into Eq. (5.1),

$$\omega^2 \propto \sum_{r=1}^{\infty} \frac{\sin[kr/2]^2}{r^3}, \tag{5.4}$$

where we have defined $r \equiv na$ and have set $m_e = e_0 = 1$ for simplicity. Thus, it is our primary task to carry out the infinite summation of Eq. (5.4). Hitherto, the most common approaches have been numerical, using methods such as the Ewald summation technique,[6] where a solution is presented in terms of rapidly converging sums. We make use of the polylogarithm function $\mathrm{Li}_n(z)$ also known as the de Jonquires function, defined as[13]

$$\mathrm{Li}_n(z) = \sum_{k=1}^{\infty} \frac{z^k}{k^n}. \tag{5.5}$$

This definition may be extended to all of the complex plane through analytic continuation, therefore we apply Eq. (5.5) to the summation of Eq. (5.4) yielding

$$\omega_{1\mathrm{D}}(k) \propto \sum_{r=1}^{\infty} \frac{\sin[kr/2]^2}{r^3} = \frac{1}{2}[-\mathrm{Li}_3(e^{-ik}) - \mathrm{Li}_3(e^{ik}) + 2\zeta(3)], \tag{5.6}$$

where $\zeta(x)$ is the Reimann zeta function. At long wavelengths the polylogarithms can be expanded to the lowest order, yielding

$$\omega_{1\mathrm{D}}(k) \approx |k| \ln^{1/2}[1/|k|]. \tag{5.7}$$

Let us turn our attention to the two-dimensional case, for which Eq. (5.1) can be generalized to a double summation over a tensor. The effect of the double summation will reduce the power of r in the denominator equation (5.6). Thus, the dominant contribution to the longitudinal eigenmode is the following sum, irrespective of whether we consider a triangular lattice or a square lattice

$$\omega_{2\mathrm{D}}(k) \propto \sum_{r=1}^{\infty} \frac{\sin[kr/2]^2}{r^2} = \frac{1}{12}[\pi^2 - 3\mathrm{Li}_2(e^{-ik}) - 3\mathrm{Li}_2(e^{ik})]. \tag{5.8}$$

We can further simplify this expression by making use of the following identity:

$$\mathrm{Cl}_n(x) = \begin{cases} \frac{1}{2} i[\mathrm{Li}_n(e^{-ix}) - \mathrm{Li}_n(e^{ix})] \to n \text{ even}, \\ \frac{1}{2}[\mathrm{Li}_n(e^{-ix}) + \mathrm{Li}_n(e^{ix})] \to n \text{ odd}, \end{cases} \tag{5.9}$$

where $\mathrm{Cl}_n(x)$ are Clausen functions[13] for a given n. It is known from functional analysis that certain Clausen functions have an exactly summable representation for arguments in a restricted range.[13] In particular, for $0 \leqslant k \leqslant 2\pi$,

$$\mathrm{Cl}_2(k) = \frac{\pi^2}{6} - \frac{\pi k}{2} + \frac{k^2}{4}. \tag{5.10}$$

Apparently, the periodicity of our system guarantees that the values of k are restricted to the first Brillouin zone. There-

fore, a more convenient representation of the 2D longitudinal plasma dispersion relation becomes

$$\omega_{2D}(k) \propto \sqrt{\frac{\pi|k|}{2} - \frac{k^2}{4}}. \tag{5.11}$$

Apparently the long wavelength behavior reduces to

$$\omega_{2D}(|k|) \propto \sqrt{|k|}. \tag{5.12}$$

If we place this derivation in the context of earlier work, this classical result can be compared to the attempts by other authors using a quantum-mechanical treatment of charged collective modes with long-range interactions. Until now, no exact analytical results exist for the classical plasmon dispersion relations of Wigner crystals in any dimension. Gold and Ghazali[14] examined a correlated quasi-1D electron system by using the random phase approximation (RPA). In the RPA treatment the authors remedy the diverging Fourier transform of the $1/r$ potential in 1D by phenomenologically adding a small but finite system width d that leads to a logarithmic part of the interaction, separating the short-ranged behavior from the long-ranged one. The resulting charged modes have the following dispersion:

$$\omega_{RPA}(k) \approx \frac{2e_0}{\sqrt{\pi}}\sqrt{v_f}|k|\ln^{1/2}\left(\frac{1}{kd}\right), \tag{5.13}$$

where v_f is the Fermi velocity. Clearly a notable difference between our classical result (5.6) and the RPA result (5.13) is the logarithmic singularity in the limit $d \to 0$, of which is a direct consequence of the authors considering a quasi-1D system rather than the purely 1D system that we have just discussed. Although our exact result contains extra dispersive curvature at values of k near the Brillouin zone boundary, our classical summation technique agrees with the RPA result's long-wavelength behavior.

Still, others have attempted to describe 1D WC behavior in the limit of an elastic Hamiltonian such as in the Luttinger liquid phase.[11] The Luttinger liquid arises as an instability in a 1D electron system with strong short-ranged interactions, captured by the Hubbard Hamiltonian. Again they contend that the true long-range behavior of the Coulomb interaction is not important aside from these minor logarithmic correction factors that modify the elastic modes to produce a dispersion relation that has the same behavior as the RPA result (5.13). A comparison is show in Fig. 7.

In 2D, until now there have been no analytical results for the precise behavior of the longitudinal plasma eigenmode. The Ewald technique has been numerically implemented by previous authors.[15,16] They discovered an unusual $\omega(k) \sim \sqrt{k}$ dependence arising strictly from the long-ranged interactions, as it is known that short-ranged interactions produce a linear phonon dispersive form. We compare our closed form result with the Ewald summation technique in Fig. 8. Evidently, there is excellent agreement.

B. The disordered systems

In the presence of disorder, the equilibrium state is, as noted above, no longer a perfect crystal, and the elementary

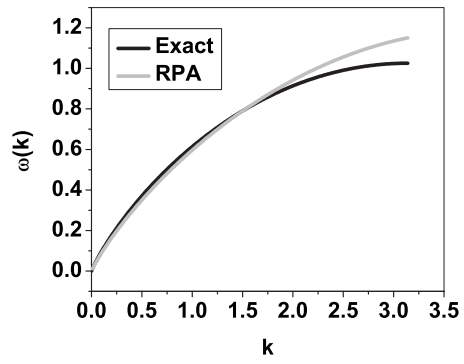

FIG. 7. A comparison of the exact 1D classical dispersion with the RPA result.

excitations are no longer plane wave modes. In fact, it is known that conditions may prevail in which some or all of those excitations are spatially localized.[17] The localization properties of the plasma eigenstates of models A and B have been explored in detail by the authors of this paper,[18] where they reported a vibrational delocalization transition at lower eigenfrequencies in model A, in that plasma modes, are localized above, and extended below, a threshold frequency. By contrast, no such transition observed in model B, in which disorder serves to localize all plasma modes. Additionally, they performed a finite size analysis of the transition in model A, yielding scaling behavior of the relative interaction strength $\kappa \equiv Q^2/J$ and an approximate value of the correlation length exponent. In this section we will focus on other aspects of the plasma eigenstates. In particular, we will explore multifractal properties of the participation moments, the electronic compressibility of the pure and disordered systems, and the frequency dependent behavior of the ac conductivity.

An important physical quantity associated with spatially localized eigenfunctions is the participation ratio P_q^j (Ref. 19) of a given moment q, defined as

$$P_q^j = \frac{1}{\sum_{k=1}^{L} |u_k^j|^{2q}}, \tag{5.14}$$

where u_k^j is the amplitude of the jth plasma eigenmode at site k.

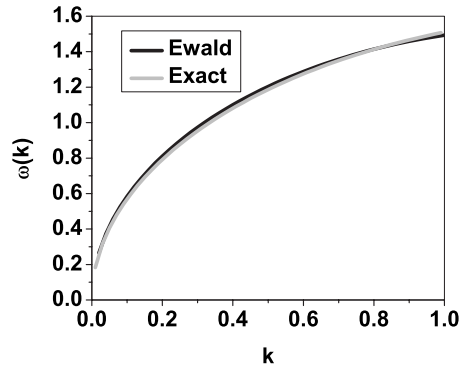

FIG. 8. A comparison of the exact 2D longitudinal dispersion with the Ewald result.

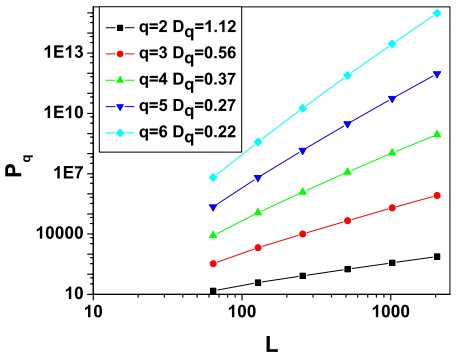

FIG. 9. (Color online) Averaged participation moments showing multifractal scaling, model A.

For this particular quantity one must account for the numerical and statistical uncertainties on finite length chains that scale as $1/\sqrt{L}$. One can smooth out the fluctuations of P_q^j by summing over all the eigenstates and ensemble-averaging over several realizations of disorder (represented by the overline bar). This yields the following length dependent quantity for finite-sized systems:

$$\overline{P_q(L)} = \frac{1}{L}\overline{\sum_{j=1}^{L} P_q^j}. \tag{5.15}$$

For the 3D Anderson model the critical scaling properties of $\overline{P_q(L)}$ were derived by Wegner[19] using renormalization group arguments in a $2+\epsilon$ expansion of the two particle spectral function of a system of interacting Q matrices. The common view is that all models exhibiting an Anderson transition will possess critical eigenfunctions that can be used to construct the quantity $\overline{P_q(L)}$, having a length dependence that scales as

$$\overline{P_q(L)} \propto L^{D_q(q-1)} \tag{5.16}$$

or, in other words, $\overline{P_q(L)}$ exhibits multifractal scaling, in that one obtains a different exponent D_q for each moment q. Other authors such as Lima *et al.* have related this scaling behavior to the wave-packet dynamics of the power-law bond disordered one-dimensional Anderson model with hopping amplitudes decreasing as $H_{nm} \propto |n-m|^{-\alpha}$. They were able to extract a time-dependent scaling analysis of the participation moments by performing a finite size scaling analysis of the electronic return probability.[20] Furthermore, they report an asymptotic value of $D_\infty = 0.5$. We have performed a similar calculation shown in Fig. 9. Indeed, the critical eigenfunctions of model A exhibit multifractal behavior. However, the asymptotic value $D_\infty \approx 0.2$, differs from the value 0.5 obtained in the analogous electronic tight-binding system.

The behavior of the plasma oscillations have further significance for physical quantities such as the electron compressibility B_T. We remark that our definition of B_T only includes the electron gas itself and does not consider the compensating background. One major reason for using this definition is that the neutralizing background contribution does not enter into the experimentally determined values of B_T when using the standard capacitive techniques, of which have been widely applied to measure the compressibility of interacting electron systems in semiconductor heterostructures.[21] B_T can be related to the volume fluctuations of a system around its average value by the relation

$$B_T \propto \frac{\langle (\Delta V)^2 \rangle}{\langle V \rangle}. \tag{5.17}$$

It follows that one can associate the normal modes $u(x)$ with these volume fluctuations in a finite system

$$B_T \propto \frac{1}{L}\left\langle \sum_{n=1}^{L} \frac{1}{\omega_n^2} \left(\left. \frac{\partial u}{\partial x} \right|_{x_n} \right)^2 \right\rangle, \tag{5.18}$$

where ω_n is the nth eigenfrequency and x_n labels the nth oscillator.

For the ordered—or clean—Wigner crystal, the precise behavior of the compressibility can be extracted by exploiting the spatial periodicity of the longitudinal plasma eigenfrequencies ω_L at long wavelengths;[22]

$$B_T \propto \lim_{q \to 0} \frac{q^2}{\omega_L^2(q)}. \tag{5.19}$$

Apparently, for the classical ordered system one can substitute the long wavelength form of the classical dispersion relations $\omega(k) \sim |k| \ln^{1/2}(1/k)$ into Eq. (5.19) to yield a vanishing compressibility $B_T = 0$.

For the disordered models considered in this paper, we have also applied Eq. (5.18) to models A and B at various system sizes and have observed a vanishing compressibility $B_T = 0$, in the limit of a large system for both cases. It is a useful check to also apply this definition of the compressibility for a system with short-ranged interactions. For a harmonic oscillator system with random couplings and nearest neighbor interactions we observe a finite compressibility. This appears to be consistent with a dispersion $\omega(k)$ that is linear in k, in the ordered system, of which, $B_T > 0$ via Eq. (5.19). This leads us to believe that the compressibility of the charges is dependent on the range of the interactions, not the nature of the disorder.

We emphasize that these results clarify an unsettled examination of the thermodynamic properties of disordered elastic systems in any dimension, of which has recently been subject of intense research.[23] We are confident that the methods used in this article can be extended to two dimensional systems, where a major unresolved problem is the compressibility behavior observed in 2D SI MOSFETS. Various research teams have experimentally observed a vanishing compressibility on the insulating side of the well known 2D metal-insulator transition.[24,25] There has been much speculation as to whether the insulating phase is an incompressible zero field Wigner crystal. Certain authors have suggested the use of the Gaussian variational replica method (GSM) as a viable tool for understanding disordered Wigner crystals.[5] However, it is known that these elastic models assume a continuum limit that washes out the full microscopic structural arrangement of the electrons; for example one could not discuss the distribution of nearest-neighbor spacings in a ran-

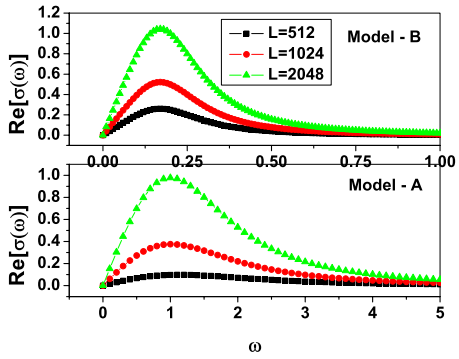

FIG. 10. (Color online) Re$[\sigma(\omega)]$ vs ω for a fixed relative disorder strength in both models κ=0.1, W_0=0.5 at different system sizes.

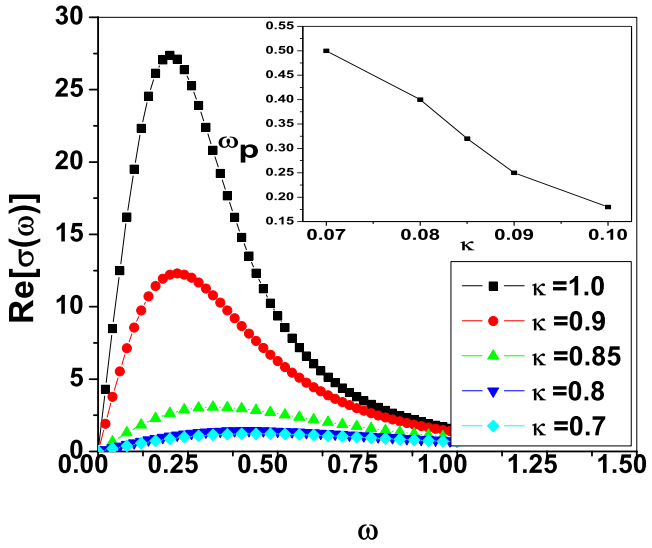

FIG. 11. (Color online) Re$[\sigma(\omega)]$ vs ω at different relative disorder strength values $\kappa(L=512)$. The inset shows the shift of the pinning frequency ω_p as the disorder is decreased.

dom charge system such as model B using the GSM, given that the spacings between nearest-neighbor particles is quantity observed only by a discrete description as we have considered in this paper. Moreover, even if one wishes to apply a continuum description, one needs to determine the elastic constants to effectively utilize the GSM method for computing the relevant physical quantities, thus rendering previous replica-based studies inconclusive. On the other hand, we have been able to calculate the compressibility by circumventing these field theoretical limitations on elastic systems (constrained by the Larkin scale) through the use of simple classical phonon methods. We hope to discuss the 2D calculations in a future article, given the fact that we have also developed some precise mathematical tools for handling the 2D long-range Coulomb interactions, of which are analogous to the exact summation in Eq. (3.1).

Another important quantity that derives from the plasma oscillations is the ac conductivity. The plasmon propagator $G(\omega)$ is itself the direct response to an external electric field interacting with the electrons. $G(\omega)$ can be determined from the Hessian or dynamical matrix, defined by Eq. (3.2), as constructed in the following resolvent:

$$G(\omega) = \sum_{R}^{L} \sum_{R'}^{L} \frac{1}{\omega^2 \mathbb{I} - D(R,R')}. \tag{5.20}$$

The ac conductivity is then given by the quantity[8]

$$\sigma(\omega) = iA\omega G(\omega). \tag{5.21}$$

The effects of disorder on the zero temperature ac transport properties was discussed by Giamarchi and Schultz[26] for 1D electron systems and Chitra *et al.* for 2D Wigner crystals.[27] With reference to this earlier work we have calculated the ac conductivity via Eq. (5.21). The finite size effects are shown in Fig. 10 for both models A and B. The key quantities of interest are the peak height H_P and its associated frequency ω_p. For the pure crystalline system ω_p corresponds to the Drude driving frequency. The disorder acts as a broadening mechanism, by which ω_p is shifted to a new frequency known as the pinning frequency and also the peak height H_P is shifted as well. We have qualitatively studied how ω_p scales with the relative interaction strength of the Coulomb potential over the random potential previously defined as κ in the critical model A. With reference to our earlier work, the observed interaction scaling in model A can be utilized to relate the critical eigenfrequency at which delocalization takes place ω_c to the pinning frequency ω_p. We have plotted the behavior of Re$[\sigma(\omega)]$ at various interaction strengths shown in Fig. 11. There is a noticeable increase in peak height with increasing interaction strength and a subtle decrease in ω_p as displayed in the window of Fig. 11. Consequently, this implies that for critical frequencies ω_c closer to the upper band edge there is a smaller pinning frequency. This can be further interpreted as connecting stronger plasma eigenmode localization with higher pinning frequencies. We remark that more careful scaling studies, both analytical and numerical must performed for a deeper understanding of the connection between critical depinning transitions and vibrational delocalization.

Another important property of the ac conductivity is the high-frequency behavior of Re$[\sigma(\omega)]$. We examined the limit $\omega \gg \omega_p$ and observed an ω dependence going as Re$[\sigma(\omega)] \sim 1/\omega^3$ for both models A and B. This is shown in Fig. 12. Certain authors have determined a universal ω^4 dependence at low frequencies for 1D disordered Wigner Crystals while others have established a ω^{2K-4} for high frequencies from renormalization group studies of interacting 1D electron systems, where K is an effective scaling coupling constant for repulsive interactions.[28] These earlier studies only consider short ranged interactions while our system takes into account the true long-ranged nature of the Coulomb interactions. The latter form would apply to our classical systems for the value $K \ll 1$, yielding a $1/\omega^4$ dependence.[26] For the purposes of comparison with similar 1D disordered electron models, our dependence on ω differs, for our results are precisely the same as the 2D system studied by Giamarchi *et al.* using the GSM technique, where they also observe Re$[\sigma(\omega)] \sim 1/\omega^3$ behavior for high frequencies.[5]

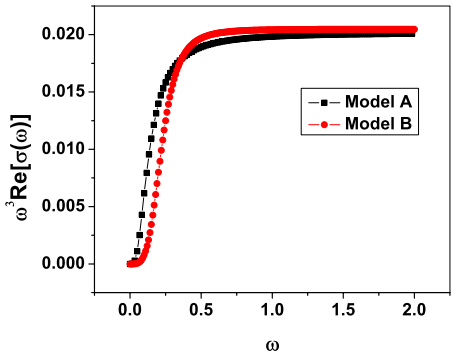

FIG. 12. (Color online) $\omega^3 \mathrm{Re}[\sigma(\omega)]$ vs ω for a fixed relative disorder strength in both models $\kappa=0.1$, $W_0=0.5$ at $L=512$. The zero slope regime at higher frequencies clearly suggests a $1/\omega^3$ dependence.

VI. CONCLUSION AND EXPERIMENTAL PROSPECTS

In this paper we have considered a wide range of phenomena in 1D disordered Wigner solids that follow from the behavior of the plasma oscillations. We have developed a mathematical formalism for studying the spatial arrangement of the particles at equilibrium as a consequence of a certain type of randomness in the Hamiltonian. We have applied probability convolutions to quantify the distribution of nearest neighbor particle spacings by assuming the particle coordinates will deviate from crystalline configuration by distances that are proportional to the total force on each particle when the system is ordered. If one adiabatically "turns on" the randomness, one can imagine the charges propagating in a viscous medium, and if the random contribution to the forces on the charges is small a linear relaxation of the particles might be expected to hold as a good approximation. We have tested this viscosity approximation against numerically relaxed ensembles, and observe what appears to be remarkably good agreement. A stronger statistical analysis will be performed in future papers that will further develop this probability convolution formalism on more rigorous grounds.

We have derived the complete dispersion relation for a longitudinal plasmon in 1D and an accurate analytical form for 2D Wigner crystals with unscreened Coulomb interactions. Our analysis introduces mathematical methods for analytically evaluating a certain class of lattice sums that have traditionally been performed numerically.

We have also explored the basic question of whether a 1DWC in the presence of quenched disorder retains its crystalline composition. We have argued that both a random potential system and a random charge system generate an internal stiffness that resists the system from completely melting in the thermodynamic limit, at least when the effect of randomness is not too great.

We briefly remark that a melting transition has been observed at a critical value of disorder strength. However, this will be formally reported in a future article.

In the process of studying models A and B numerically, we have revised existing computational paradigms for incorporating long ranged Coulomb forces in systems with periodic boundary conditions and disorder. A numerical relaxation scheme has been outlined along with a procedure for studying the collective modes of disordered Wigner crystals or other "glasslike" structures in general.

We conclude by emphasizing the necessity for experimental probes of the density response functions in order that one may investigate the possibility of a vibrational delocalization transition and our predictions of a zero compressibility phase. Glasson *et al.* have already observed Wigner crystal ordering in a quasi-1D system.[29] We consider the possibility of well-controlled manipulation of the substrate randomness as a viable avenue by which the scaling behavior of models A and B can be investigated experimentally. Furthermore, based on the observed connection between the delocalization transition and the pinning frequency ω_p, ac conductivity measurements are also quite essential for elucidating our understanding of the basic physics involved.

ACKNOWLEDGMENTS

We thank M. M. Fogler for comments on the manuscript. In addition, we acknowledge useful discussions with S. Chakravarty, Y. Tserkovnyak, and S. E. Brown.

APPENDIX A: THE DISTRIBUTION OF RANDOM CHARGE PRODUCTS

In general, the charge product density function is given as a convolution of two different densities[30]

$$P(t) = \int \int P_{q,i}(Q_i) P_{q,j}(Q_j) \delta(Q_i Q_j - t) dQ_i dQ_j. \quad \text{(A1)}$$

If the two charges share a common density function, then

$$P(t) = \int P_q(Q) P_q\left(\frac{t}{Q}\right) \frac{dQ}{|Q|}. \quad \text{(A2)}$$

The range of values for t must be carefully determined for various regimes, depending on the type and width of distribution $P_q(Q_i)$. We start by examining the case of a uniform distribution of random single charges in model B, in which

$$P_q(Q) = \begin{cases} \dfrac{1}{W_2 - W_1}, & W_1 < Q < W_2, \\ 0 & \text{otherwise}. \end{cases} \quad \text{(A3)}$$

Evidently, nucleons and electrons can only have integer values of the charge e, so this particular distribution is unphysical and unrealistic. However, we consider this distribution only as a version of a randomly distributed coupling constant and for the purposes of determining which features of the system are robust with respect to distribution type.

After determining the range of values for t, we can solve for the joint distribution for a product of charges

$$P(t) = \begin{cases} \dfrac{\ln|t/W_1^2|}{(W_2 - W_1)}, & t < W_2 W_1, \\ \dfrac{\ln|W_2^2/t|}{(W_2 - W_1)}, & t > W_2 W_1. \end{cases} \tag{A4}$$

As a more germane alternative, we also consider a binary distribution for model B, defined as simply a sum of two delta functions with equal statistical weights. This particular type of disorder can be interpreted as a form of chemical disorder or a type of binary alloy. We consider the binding of chemical constituents to the Wigner crystal such that there are effectively two values of charges random distributed throughout the system:

$$P_q(Q) = \frac{1}{2}\delta(Q - Q_1) + \frac{1}{2}\delta(Q - Q_2). \tag{A5}$$

The product distribution simply consists of three peaks at the values Q_1^2, $Q_1 \times Q_2$, and Q_2^2.

$$P(t) = \frac{1}{4}\delta(Q_1^2 - t) + \frac{1}{2}\delta(Q_1 Q_2 - t) + \frac{1}{4}\delta(Q_2^2 - t). \tag{A6}$$

Finally, we consider the Gaussian product distribution

$$P(t) = \int_{-\infty}^{\infty}\int_{\infty}^{\infty} e^{-(Q_i - \mu)^2/2\sigma_i} e^{-(Q_j - \mu)^2/2\sigma_j}(Q_i Q_j - t) dQ_i dQ_j. \tag{A7}$$

For $\mu = 0$ this integral can be evaluated exactly to yield

$$P(t) = \left(\frac{1}{\pi\sigma^2}\right) K_0\left(\frac{|t|}{\sigma^2}\right), \tag{A8}$$

where K_0 is a modified Bessel function of the second kind.[13] For a nonzero mean the product distribution can be determined numerically.

APPENDIX B: THE EWALD SUMMATION OF A QUASI-1D PERIODIC SYSTEM

We carry out the Ewald summation technique for a quasi-1D system of charges in a uniform neutralizing background. The electrostatic potential of interest has the following form:

$$\frac{1}{|r - nL|} - \int \frac{dx/L}{\sqrt{(r-x)^2 + b^2}}. \tag{B1}$$

The first term can be expanded out as an integral:

$$\frac{1}{|r - nL|} = \int_0^{\infty} e^{-t(r - nL)^2} t^{-1/2} dt.$$

This integral can be broken up into two parts by introducing a suitable cutoff $\frac{\pi\beta}{L^2}$:

$$= \int_0^{\pi\beta/L^2} e^{-t(r - nL)^2} t^{-1/2} dt + \int_{\pi\beta/L^2}^{\infty} e^{-t(r - nL)^2} t^{-1/2} dt.$$

The second integral can be evaluated through a variable substitution and can be left as is:

$$t \to \frac{\pi x}{L^2} \Rightarrow \sum_{n=-\infty}^{\infty} \int_{\beta}^{\infty} \frac{\sqrt{\pi}}{L} e^{-\pi x (r/L - n)^2} x^{-1/2} dx.$$

Next, we apply the Poisson sum formula to the first integral

$$= \sum_{m=-\infty}^{\infty} \int_0^{\pi\beta/L^2} \int_{-\infty}^{\infty} e^{2\pi i m n} e^{-t(r - nL)} t^{-1/2} dn dt.$$

The integral on n can be carried out by a standard completion of the squares trick yielding

$$= \sum_{m=-\infty}^{\infty} \frac{\sqrt{\pi}}{L} \int_0^{\pi\beta L^2} e^{(2\pi i r m/L) - (\pi^2 m^2/L^2 t)} \frac{dt}{t}.$$

It is important that we properly subtract the divergent contribution of the $m=0$ term. The resulting summand contains a lower incomplete gamma function

$$= \sum_{m \neq 0}^{\infty} e^{(2\pi i r m/L)} \Gamma\left(0, \frac{m^2 \pi}{\beta}\right).$$

Lastly we subtract the divergent contribution at $m=0$ arising from the neutralizing background

$$\int \frac{dx/L}{\sqrt{(r-x)^2 + b^2}} = \int_0^{\infty} \int \frac{dx}{L} e^{-[(r-x)^2 + b^2]t} t^{-1/2} dt.$$

If we include the other $m=0$ term from the previous summand the contributions to the sum become

$$\int_0^{\pi\beta/L^2} (1 - e^{b^2 t}) \frac{dt}{t} + \int_{\pi\beta/L^2}^{\infty} e^{b^2 t} \frac{dt}{t} \approx \ln\beta + C,$$

where C is some constant. Our final expression for the long-ranged electrostatic potential becomes

$$V(r) = \sum_{n=-\infty}^{\infty} \int_{\beta}^{\infty} e^{\pi x (r/L - n)^2} x^{1/2} dx + \sum_{m \neq 0} e^{2\pi i m r/L} \Gamma\left(0, \frac{m^2 \pi}{\beta}\right) - \ln(\beta). \tag{B2}$$

It is important to note that the expression converges to a value that is independent of the cutoff β.

APPENDIX C: THE BAND STRUCTURE FOR POWER LAW HOPPING

The tight-binding Hamiltonian of interest takes form

$$H = \sum_{i}^{L} \varepsilon_0 |i\rangle\langle i| + \sum_{\langle ij \rangle}^{L} t_{ij}(|i\rangle\langle j| + |j\rangle\langle i|), \tag{C1}$$

where $\langle ij \rangle$ denotes a sum over all unique pairs of lattice sites i and j. For simplicity we have assumed only one orbital per site. The hopping matrix elements t_{ij} have the power law dependence

$$t_{ij} = \frac{t_0}{|i-j|^{\beta}}. \tag{C2}$$

Evidently, the Hamiltonian satisfies the time-independent Schrodinger equation $H|\psi_k\rangle = E(k)|\psi_k\rangle$. Furthermore, for translationally invariant systems, we can make use of the Fourier transform, having the form $|\psi_k\rangle = \sum_{l'} e^{ikl'}|l'\rangle$, with $l = 1,2,\ldots$. We can apply this ansatz along with Eq. (C1) to the Schrodinger Eq. (C1) to yield the following expression:

$$H|\psi_k\rangle = \sum_{l'} e^{ikl'}|l'\rangle \left\{ \sum_{r=1}^{\infty} \frac{t_0(\cos[kr]-1)}{r^{\beta}} + \varepsilon_0 \right\}$$

$$= \sum_{l'} e^{ikl'}|l'\rangle \{t_0(\mathrm{Li}_{\beta}[e^{ik}] + \mathrm{Li}_{\beta}[e^{-ik}]) + \varepsilon_0\}, \tag{C3}$$

where we have defined $r=|i-j|$ and we have also absorbed various constants into the definition of t_0 and ϵ_0. Again we made use of the polylogarithm function $\mathrm{Li}_n(z)$ and following similar steps as before our final expression for the energy dispersion relation reduces to

$$E^{\beta}(k) = t_0(\mathrm{Li}_{\beta}[e^{ik}] + \mathrm{Li}_{\beta}[e^{-ik}]) + \varepsilon_0. \tag{C4}$$

Equation (C4) is general to a particular exponent β, and one must properly consider the odd and even cases in order to determine when it is appropriate to use a particular Clausen function. More specifically, for odd powers of β one may use Eq. (5.9) reducing the final energy dispersion to

$$E^{\beta}(k) = 2t_0 Cl_{\beta}[k] + \varepsilon_0 \tag{C5}$$

for $\beta = 2n+1$; $n = ,0,1,2,\ldots$.

*shimul@physics.ucla.edu
†jrudnick@physics.ucla.edu

[1] E. Wigner, Phys. Rev. **46**, 1002 (1934).
[2] B. I. Shklovskii, Phys. Rev. Lett. **82**, 3268 (1999).
[3] T. Giamarchi and P. Le Doussal, Phys. Rev. Lett. **72**, 1530 (1994).
[4] J. M. Ziman, *Models of Disorder* (Cambridge University Press, Cambridge, 1979), Chap. 2.
[5] R. Chitra, T. Giamarchi, and P. L. Doussal, Phys. Rev. B **65**, 035312 (2002).
[6] P. P. Ewald, Ann. Phys. **369** (3), 253 (1921).
[7] W. H. Press, *Numerical Recipes in C++: The Art of Scientific Computing*, 2nd ed. (Cambridge University Press, Cambridge, 2002).
[8] N. W. Ashcroft and N. D. Mermin, *Solid State Physics* (Holt Rinehart and Winston, New York, 1976).
[9] A. Alastuey and B. Jancovici, J. Stat. Phys. **24**, 443 (1981).
[10] G. Piacente, I. V. Schweigert, J. J. Betouras, and F. M. Peeters, Phys. Rev. B **69**, 045324 (2004).
[11] H. J. Schulz, Phys. Rev. Lett. **71**, 1864 (1993).
[12] G. Piacente, F. M. Peeters, and J. J. Betouras, Phys. Rev. E **70**, 036406 (2004).
[13] M. Abramowitz and I. A. Stegun, *Handbook of Mathematical Functions* (Dover Publications, New York, 1970).
[14] A. Gold and A. Ghazali, Phys. Rev. B **41**, 7626 (1990).
[15] L. Bonsall and A. A. Maradudin, Phys. Rev. B **15**, 1959 (1977).
[16] R. S. Crandall, Phys. Rev. A **8**, 2136 (1973).
[17] P. W. Anderson, Phys. Rev. **109**, 1492 (1958).
[18] S. Akhanjee and J. Rudnick, Phys. Rev. B **75**, 012302 (2007).
[19] F. Wegner, Z. Phys. B **36**, 209 (1980).
[20] R. P. A. Lima, F. A. B. F. de Moura, M. L. Lyra, and H. N. Nazareno, Phys. Rev. B **71**, 235112 (2005).
[21] J. P. Eisenstein, L. N. Pfeiffer, and K. W. West, Phys. Rev. B **50**, 1760 (1994).
[22] P. C. Martin, *Measurements and Correlation Functions* (Gordon and Breach Science Publishers, New York, 1968).
[23] G. Schehr, T. Giamarchi, and P. L. Doussal, Phys. Rev. Lett. **91**, 117002 (2003).
[24] S. C. Dultz and H. W. Jiang, Phys. Rev. Lett. **84**, 4689 (2000).
[25] G. Allison, E. A. Galaktionov, A. K. Savchenko, S. S. Safonov, M. M. Fogler, M. Y. Simmons, and D. A. Ritchie, Phys. Rev. Lett. **96**, 216407 (2006).
[26] T. Giamarchi and H. J. Schulz, Phys. Rev. B **37**, 325 (1988).
[27] R. Chitra and T. Giamarchi, Eur. Phys. J. B **44**, 455 (2005).
[28] M. M. Fogler, Phys. Rev. Lett. **88**, 186402 (2002).
[29] P. Glasson, V. Dotsenko, P. Fozooni, M. J. Lea, W. Bailey, G. Papageorgiou, S. E. Andresen, and A. Kristensen, Phys. Rev. Lett. **87**, 176802 (2001).
[30] M. Evans, N. Hastings, and B. Peacock, *Statistical Distributions* (Wiley, New York, 2000).